ELSEVIER

PII: S0032-3861(96)00818-X

Polymer Vol. 38 No. 11, pp. 2617–2625, 1997

0032-3861/97/$17.00 + 0.00

Scanning force microscopy of poly(ethylene terephthalate) surfaces: comparison of SEM with SFM topographical, lateral force and force modulation data

John S. G. Ling and Graham J. Leggett*
Department of Materials Engineering and Materials Design, The University of Nottingham, University Park, Nottingham NG7 2RD, UK
(Received 27 June 1996)

Biaxially oriented poly(ethylene terephthalate) films have been characterized using scanning force microscopy (SFM). Comparison of SFM topographical and SEM data revealed that the SFM provides superior lateral resolution and direct access to height data. Structural details absent from the SEM images were revealed by SFM, including radiating features observed around the silicate inclusions, tentatively attributed to local strain-induced crystallization. Lateral force microscopy (LFM) revealed high contrast on the surfaces of the silicate additives in the forwards scan direction, and inverted contrast in the reverse direction, indicating a substantial and unexpected friction interaction between the SFM tip and the silicate particles. Force modulation microscopy (FMM) images exhibited unexpectedly low contrast for the silicates, while the perimeters of silicate particles were found to be delineated with striking clarity. FMM contrast was sharply dependent on imaging parameters, including, in particular, the amplitude of oscillation and the scan speed. © 1997 Elsevier Science Ltd.

(Keywords: poly(ethylene terephthalate); scanning force microscopy; surfaces)

INTRODUCTION

The past two decades have seen substantial advances in our ability to characterize polymer surfaces using spectroscopic techniques. However, in many applications, such as adhesion, it has not been possible to separate the influence of polymer surface chemistry from that of surface topography. Traditionally, electron microscopies have been used to examine the topography and structure of polymer films. However, the interrogation of polymer surfaces by electron microscopy presents a number of scientific challenges which relate to the electron beam–sample interaction. First, polymers are very sensitive to bombardment-induced damage and chemical and physical changes readily occur on beam exposure. Second, the poor electrical conductivity of most polymers means that appropriate pre-preparation (for example the deposition of a conducting coating) needs to be employed in order to minimize electrostatic charging. Third, the low atomic numbers of the elements typical of polymeric materials means that electrons are scattered only weakly causing low image contrast[1]. The application of a conducting coating (for example gold) may therefore help to improve contrast too. Surface replication techniques also assist with sample inspection but necessarily provide mainly morphological data. Heavy metal staining has been widely used in biological microscopy studies in order to explicate compositional variations. The selective adsorption of the staining agent in amorphous rather than crystalline regions of a polymer structure is useful in examining the distribution of ordered and disordered phases within the polymer, although some polymers respond better to staining agents than others.

The advent of scanning probe microscopy (SPM) and, in particular, scanning force microscopy (SFM) offers considerable potential to deepen our understanding of the surface structures of polymeric materials through the facilitation of improved resolution in topographical investigations and, perhaps more importantly, through the investigation of local properties. SFM facilitates the realization of exceptional resolution, often without the need for intricate sample preparation, and in certain instances features on the molecular scale have been resolved in polymeric systems. Lin and Meier[2] have reported images of oriented polyethylene samples in which what appear to be individual molecular chain-folds may be observed, providing direct confirmation of the generally accepted model for the microstructure of drawn semicrystalline thermoplastics. Stocker *et al.* claim to have observed right and left helical conformations of epitaxially crystallized syndiotactic polypropylene[3], and Magonov and Cantow[4] have published images of the surfaces of crystalline and semicrystalline polymers. However they have reported that amorphous atomic arrangements are difficult to separate from experimental noise. Miles *et al.*[5] have investigated melt-spun

*To whom correspondence should be addressed. Tel: +44 115 9513748. Fax: +44 115 9513741. E-mail: Graham.Leggett@Nottingham.ac.uk

polymer surfaces and have reported that shish-kebab structures may be observed in images of polyethylene films. In general, however, examples of lateral resolution superior to that offered by transmission electron microscopy are rare; more significant is the direct access to topographical information provided by SFM and the potential offered for probing local properties.

Early local property investigations by SPM were directed towards the characterization of electronic structure[6]. More recently, force interactions have been measured between functionalized tips and flat surfaces. In these measurements, the SFM is employed in a manner analagous to the classical surface forces apparatus, but in a localized fashion. Ducker *et al.*[7] have measured the force between a single colloidal sphere, attached to the SFM tip, and a planar silica surface. Lee *et al.*[8,9] have functionalized spherical silica probes with biotinylated bovine serum albumin[8] and DNA oligomers[9], and measured the strength of their interactions with a streptavidin surface and a surface functionalized with DNA oligomers, respectively. In this way, the strengths of molecular recognition processes may be investigated directly. Besides force–distance measurement, other SFM techniques have been developed which are potentially promising means by which local polymer surface properties may be investigated. In frictional or lateral force microscopy (LFM), the torsional or lateral twisting motions of the cantilever are recorded with high contrast, and are regarded as being indicative of significant frictional interactions between tip and sample. LFM has been employed to image a variety of materials including patterned self-assembled monolayers[10], Langmuir–Blodgett films[11] and polymer crystals[12]. High surface energies in model materials are found to give rise to high contrast, confirming the expected form of behaviour. In studies of polyoxymethylene[12] and polyethylene[13] single crystals, Nisman *et al.* observed contrast differences between fold domains of the crystal surface, which they attributed to changes of the directionality of the chain folds in the fold plane. However, where samples exhibit significant topographical variations, contrast is clearly likely to be the consequence of the complex convolution of lateral and normal force interactions.

Force modulation microscopy (FMM) utilizes an oscillating probe in contact with the sample surface to attempt to probe local mechanical properties. The amplitude of oscillation is low compared to a tapping mode and the frequency of oscillation is substantially lower than the resonant frequency of the cantilever (typically of the order of a few kHz compared to typical resonant frequencies for commercial microfabricated cantilevers in the range 10–100 kHz). The rate of increase of the interaction force with decreasing nominal tip-sample separation is measured, with high dF/ds values leading to high image contrast. High contrast is therefore typically equated with high stiffness. Maivald *et al.* have demonstrated the efficacy of FMM in the case of carbon fibre/epoxy composites[14]. FMM is one of a number of modulation techniques which are currently being explored; for example, Burnham *et al.* have explored the use of high frequency cantilever oscillation with the development of scanning local-acceleration microscopy, SLAM[15].

In the present work, we report studies of commercially produced polyester films by scanning force microscopy. Industrially produced materials have, as yet, received relatively little attention in the SFM literature although scanning probe techniques offer potentially valuable data relating to their morphologies and the influence of film processing operations. In particular, we have examined a material treated to incorporate silicate additives at the surface. We have compared SFM topographical and SEM images and have explored LFM and FMM techniques. Our primary concern is to evaluate the nature of the information provided by SFM for these materials, and to elucidate the factors which control image contrast.

EXPERIMENTAL

Samples of Mylar D were obtained from Goodfellow Advanced Materials (Cambridge, UK) and were used as received. Mylar D is a commercial biaxially oriented poly(ethylene terephthalate) (PET) film produced by Du Pont. Samples of biaxially oriented O grade Melinex (for comparative X.p.s. characterization) were supplied by Professor D. Briggs (ICI, Wilton, UK), with two clean sides facing and were used as received. Colloidal gold was obtained from Agar (Stansted, UK) at a concentration of 7×10^{21} particles cm^{-3}, and diluted by a factor of 5 using reverse osmosis water, before deposition onto freshly cleaved mica (Agar) and drying by evaporation in air. The nominal gold particle diameter was 21.3 nm.

Scanning electron microscopy (SEM) was performed using a Jeol 6400 SEM on samples pretreated by the deposition of a layer of sputtered gold. To reduce surface damage, the accelerating voltage in the SEM was set at 15 kV with a working distance of 12 mm and a spot diameter of 30 nm.

Scanning force microscopy (SFM) was performed in contact mode using a TopoMetrix Explorer scanning probe microscope (TopoMetrix Corporation, Saffron Walden, UK). Images were recorded under ambient conditions using commercially fabricated pyramidal silicon nitride tips (Topometrix Corporation) attached to 2 or 15 μm heads and having nominal force constants of either 0.032 or 0.064 N m^{-1}. Typical imaging forces were estimated to lie in the range 1–10 nN. Topographical, LFM and FMM images were recorded. Using the Explorer software, LFM and topographical images could be recorded simultaneously.

RESULTS AND DISCUSSION

Comparison of topographical SFM and SEM

One of the advantages offered by SFM when compared to electron microscopy is the possibility of direct access to the surface topography. While electron microscopy may yield data which are highly resolved in the lateral plane, the complexity of the mechanism of image contrast formation means that the determination of topographical data from the observed contrast is difficult. In constant force mode SFM, the sample topography is readily determined, and *Figure 1* shows a representative image of a region of a Mylar D sample. *Figure 2* shows an SEM image of a Mylar sample that has first been coated with a layer of sputter-deposited gold. The silicate additive particles may be observed as globular features in both images. An average interparticle spacing of some 500 nm is observed. Examination of

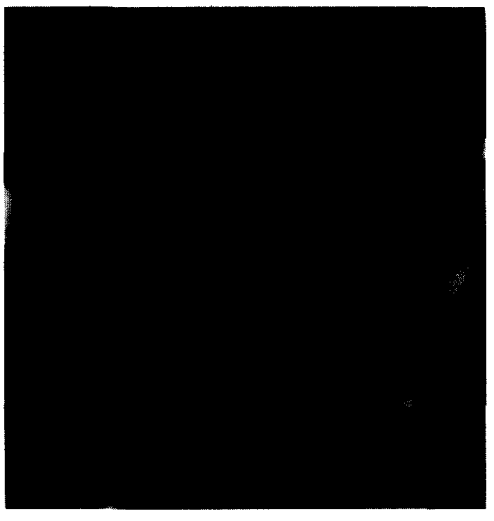

Figure 1 Topographical SFM image of a region of a Mylar D sample. Image size: $3\mu m \times 3\mu m$

Figure 2 SEM image of a gold-coated Mylar D sample

line profiles through the globular features observed in the SFM images reveals that the silicate particles (see *Figure 3* for a representative example) typically prodtrude some 20–40 nm above the polymer film surface, and exhibit diameters at the surface which lie in the range 100–500 nm. These measurements of particle diameters are in close agreement with the results of the SEM investigation. There is no parallel in the SEM data with the measurement of particle heights. However, the accuracy of height measurement on our instrument has been confirmed by studies of monodispersed colloidal gold particles with diameters in this range (which have been determined accurately using transmission electron microscopy).

The silicate particles were found to exhibit similar morphologies in both the SFM and the SEM images. However, there were some differences in detail. Generally speaking, the silicates were more crisply resolved in the SFM topographical images. Furthermore, greater structural detail was observed in the SFM images, which suggested that some of the larger features are in fact clusters of smaller particles. Boundaries between the individual components of these clusters were clearly resolved using force modulation techniques (see below),

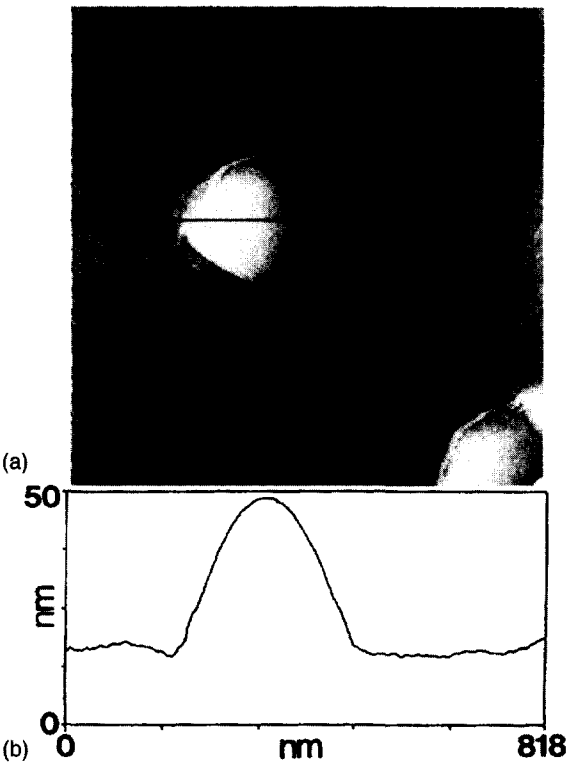

Figure 3 Topographical SFM image of a single silicate particle (a) and a line profile through the additive (b), showing exact topographical data

although they were somewhat less readily identified in the topographical images.

Radiating features were observed around some of the larger features in the SFM topographical images and were of particular interest. These features were not observed in the SEM micrographs, but were reproducibly and regularly observed in SFM images. Preliminary results using non-contact SFM have confirmed that these radiating features are polymer surface structures and are not produced by the SFM tip–surface interaction[16]. We do not have a full explanation for the observation of these features at present. However, one possible explanation is that they are the result of local strain-induced crystallization around the silicate additives. Inclusion of the silicate particles will cause deformation of the polymer surface; the associated strain may be sufficient to cause crystallization of material close to the additive. We are presently investigating this phenomenon in greater detail.

Lateral force microscopy

Figure 4 compares LFM and topographical SFM images of a region of a Mylar D sample recorded simultaneously. *Figure 5* shows an LFM image of a single silicate particle, the corresponding topographical image of which is shown in *Figure 3*. The LFM images (*Figures 4a* and *5*) reveal a substantial contrast difference between the surfaces of the additive particles and the surrounding polymeric material. The silicates exhibit high contrast, indicative of significant torsional motion of the cantilever as these regions are imaged. According to the simple interpretation of LFM, this implies that substantial lateral forces act on the tip as it traverses the surfaces of the silicate particles; it may therefore be inferred that the additives have a higher coefficient of

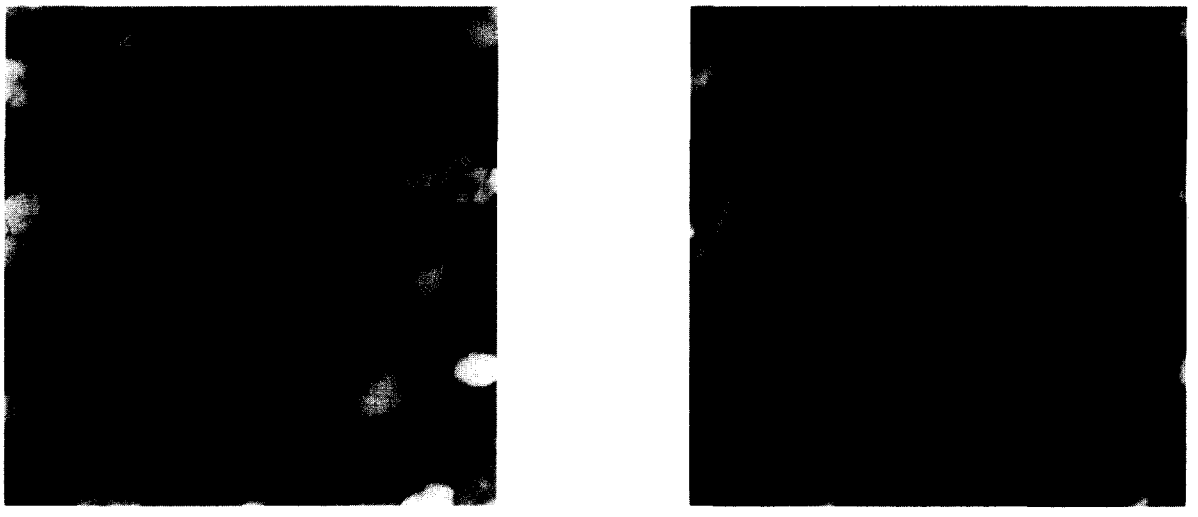

Figure 4 LFM (a) and topographical (b) images of the same region of a Mylar D sample recorded simultaneously. Image size: $3\,\mu m \times 3\,\mu m$. Scan speed: $9\,\mu m\,s^{-1}$

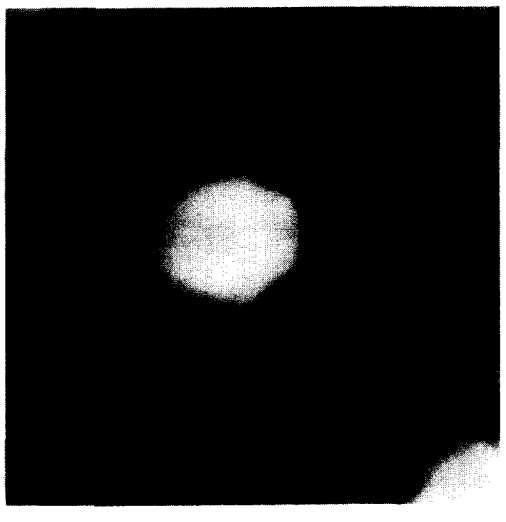

Figure 5 LFM image of a single silicate particle. The topographical image of this particle is shown in *Figure 3a*. Image size: 816×816 nm. Scan speed: $2\,\mu m\,s^{-1}$ (forwards direction)

friction than the surrounding polymeric matrix. However, care should be exercised in interpreting the data in *Figures 4* and *5*, because LFM images are influenced by a number of factors including surface chemical composition[10,11], molecular orientation[12,13], topography[17] and instrumental parameters.

Grafstrom *et al.* have provided a simple theoretical treatment of LFM which makes the connection between lateral forces and sample topography explicit[17]. According to their analysis, for a force F_N normal to the sample surface, as a consequence of the application of a load during imaging, the lateral force F_y in a direction y orthogonal to both the cantilever and the surface normal is given by

$$F_y = F_{ty} - s_y F_N \qquad (1)$$

where s_y is the slope in the y-direction and F_{ty} is the force tangential to the surface normal in the y-direction. In the limit that the surface is completely flat, the $s_y F_N$ component vanishes because $s_y = 0$. However, where there are substantial variations in topography, then the $s_y F_N$ component may become significant. It is possible, therefore, that the topography may change sufficiently while the tip traverses a silicate particle for the $s_y F_N$ component to be an important contribution to the contrast shown in *Figures 4* and *5*. In order to determine the origin of the contrast in *Figures 4* and *5*, we sought to examine the role of topography in contrast formation in two ways. First, we investigated the effect on LFM contrast of changing the scan direction, and second, we recorded LFM images of model materials which may be expected to give rise to an LFM contrast which comprises a substantial $s_y F_N$ component.

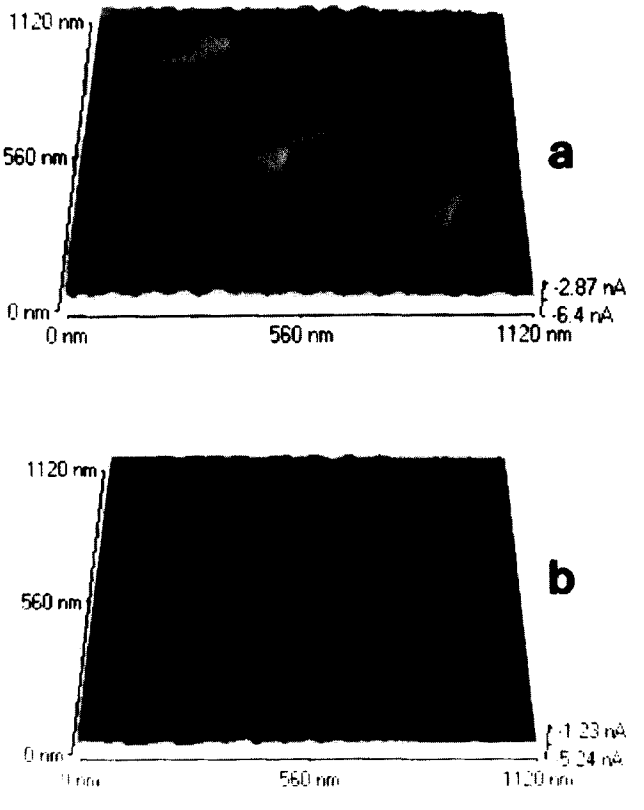

Figure 6 Comparison of LFM image contrast in the forwards and reverse directions. Image size: $1.2\,\mu m \times 1.2\,\mu m$. Scan speed: $5.5\,\mu m\,s^{-1}$

In LFM, the lateral force is determined from the difference between the signals falling on the left and right halves of the four-quadrant photo-detector. Provided the difference is determined in the same way irrespective of cantilever scan direction (for example, the magnitude of the LFM response is always the signal detected on

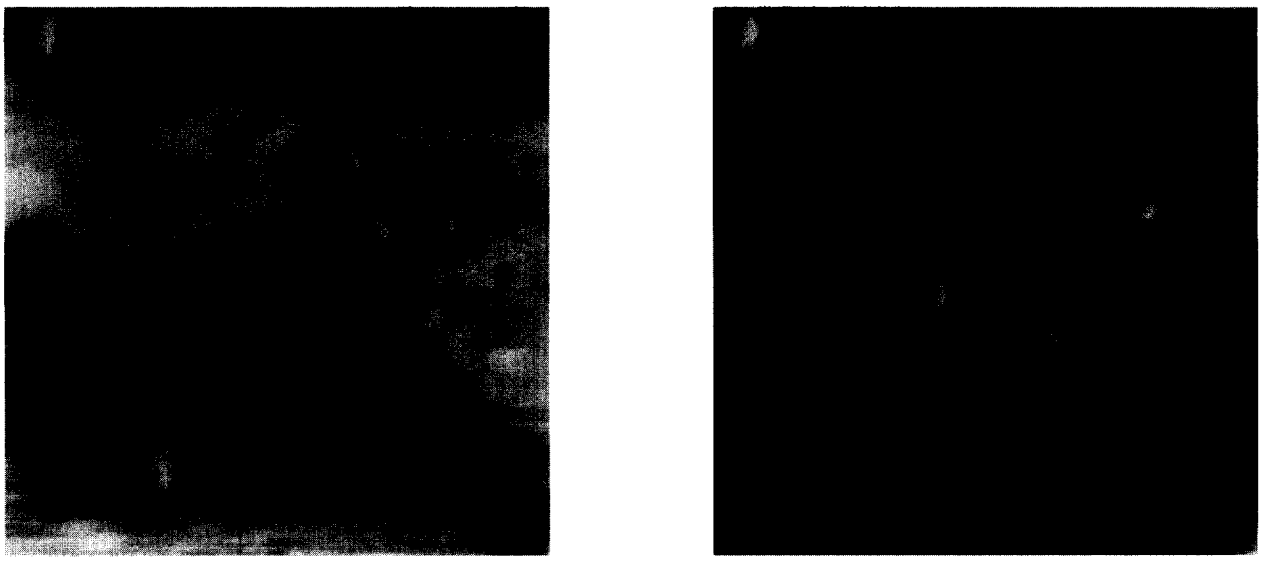

Figure 7 Forwards and reverse direction LFM images of colloidal gold particles deposited onto a cleaved mica surface. Image size: 1 μm × 1 μm

the left-hand side minus that detected on the right), then the contrast in LFM will reflect the directionality of the lateral forces measured. For a given frictional interaction, there will be a sign inversion in the lateral force on switching cantilever scan directions from left–right (forward) to right–left (reverse). In principle (given vanishing piezoelectric drift), the topographical contribution to the LFM image may be removed by subtracting images recorded in the forward and reverse directions[17]; the difference between the forward and reverse direction lateral forces is the frictional force acting between the tip and the sample[17,18]. Consequently, it is possible to straightforwardly distinguish contrast due to sample topography from contrast due to frictional interactions in LFM images, by comparing the contrast measured in the forward and reverse scanning directions.

Figure 6 shows forward and reverse LFM images of three silicate features observed on a sample of Mylar D. The contrast in *Figure 6a* is similar to that observed in *Figures 4* and *5*: relatively speaking, the silicates have higher contrast than the surrounding polymeric material. This image was, like the LFM images shown in *Figures 4* and *5*, recorded in the forwards scan direction. The image shown in *Figure 6b* was recorded in the reverse-direction, and it can be seen that a contrast inversion has occurred. The silicates, which appeared as raised features in *Figure 6a*, are observed as depressions in *Figure 6b*. This indicates that the contrast observed in the LFM images is, despite being unexpected, nevertheless likely to be the consequence of a frictional interaction between the tip and the sample. In reverse-direction imaging, the frictional force acts in the same direction with respect to the motion of the cantilever as it does in forward-direction imaging, but because the photodetector response is sensitive to directionality in the forces acting in the horizontal plane, the lateral force registers a sign change leading to a depression in the reverse-direction image when displayed as a topograph.

Further confirmation that the contrast in the LFM images is the consequence of frictional interactions comes in studies of colloidal gold particles. Particles with a mean diameter of 21.3 nm were deposited from an aqueous suspension onto freshly cleaved mica. The mica substrate provides an atomically flat surface upon which the influence of the topography of the gold particles on the LFM detector response may be explored selectively. A particle diameter of 21.3 nm was chosen because the silicate additives typically protrude some 20–40 nm above the Mylar surface.

Figure 7 shows LFM images of colloidal gold particles recorded in the forwards and reverse directions. The colloidal particles do exhibit contrast in these images; however, the contrast is essentially the same when imaged in both directions (high on the right-hand side of each particle and low on the left). This contrast is the result of variations in the force normal to the sample surface as the particles are imaged, and is not the consequence of frictional interactions. However, regions of the substrate surface do exhibit a contrast inversion. The lower region of the image shown in *Figure 7a* exhibits low contrast with respect to the portion of the image directly above it; this situation is reversed in *Figure 7b*. Furthermore, the upper region of *Figure 7a* exhibits a number of dark patches which are observed as bright patches in *Figure 7b*. These contrast inversions indicate that differential frictional responses are recorded for different regions of the mica surface, possibly the result of inhomogeneities in the surface chemical composition. The diameters observed for the gold particles in the SFM images are broadened (when compared to the expected value of 21.3 nm); this is, however, expected when sample feature sizes are smaller than the radius of curvature of the imaging tip. When the *heights* of the colloidal gold particles were compared with their diameters measured using transmission electron microscopy (no distortion of particle dimensions was expected normal to the sample surface), the agreement was found to be good.

We noticed little variation in the contrast in the LFM images of Mylar D as the scan velocity was varied over the range typically employed during imaging with our system (5–60 μm s^{-1}). Haugstad *et al.* have reported a dependence of the frictional force in LFM on scan velocity[18], but they also observed only a small change over the range of velocities which we have employed. Further studies in this laboratory will explore the scan rate dependence of the contrast in LFM in more detail over a broader range of scan velocities.

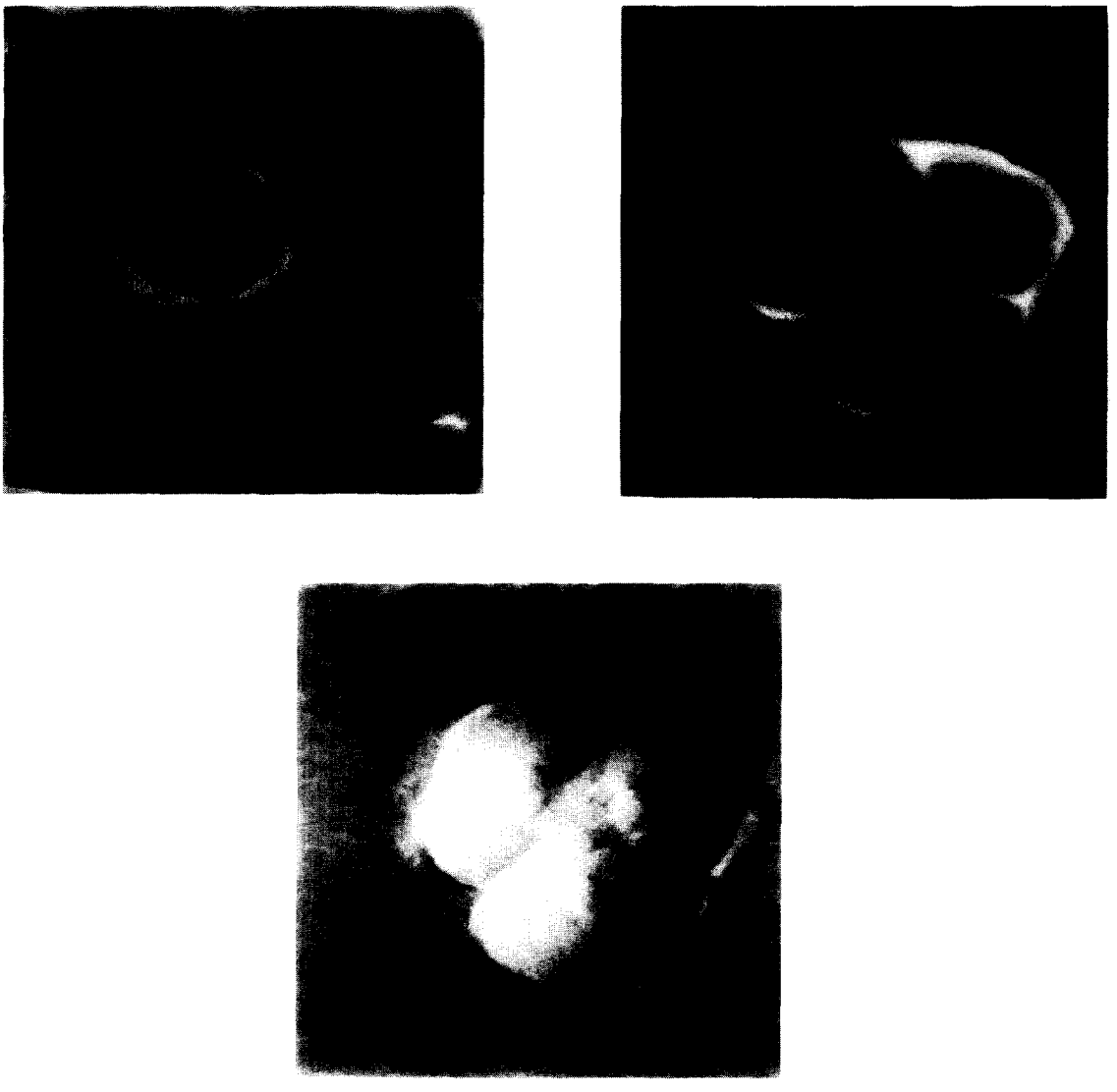

Figure 8 Force modulation images of a single silicate particle (a) and a cluster of three particles (b). The topographical image of the silicate cluster is shown in (c). Image sizes: (a) 816 nm × 816 nm; (b + c) 495 nm × 495 nm. Scan speed: 3 μm s^{-1}

Force modulation microscopy

A variety of modulation techniques have been reported for utilization in SFM. Force modulation microscopy was designed to probe the local mechanical responses of materials. In particular, by modulating the position of either the sample or the cantilever, the local response of a material may be measured under periodic compressive loading. On our instrument, the cantilever position is modulated in contact mode, although accounts in the literature generally refer to instruments in which the sample position is modulated[14,19]. The cantilever flexes giving rise to an increasing force F as the nominal tip-sample separation z decreases. High contrast arises where dF/dz is large (i.e. where the sample deforms relatively little during any given cycle), and according to the simplest interpretation of contrast in force modulation mode (FMM), the sample may be said to be stiffer in such regions[14]. Under the same imaging conditions, a softer surface will deform more extensively giving rise to lower contrast (dF/dz is small). Maivald *et al.* have imaged a carbon fibre/epoxy composite using FMM, and measured increased contrast over the fibre cross-sections compared to the surrounding resin matrix. These data are straightforwardly interpreted in terms of the variations expected in the elastic moduli of the materials concerned. Kajiyama and co-workers have used a variation of the FMM technique, termed by them scanning viscoelastic microscopy (SVM)[20–22]. Like FMM, this technique utilizes a low frequency modulation of the sample to probe local mechanical responses. These authors have applied their technique to polymer blends. By attempting to measure the photodetector signals in and out of phase with the sinusoidal oscillation applied to the sample, they have attempted to characterize the viscoelastic properties of the blends. By measuring the in-phase signal, they have observed differential contrast in phase-separated blends containing polymers above and below their glass transition temperatures, attributed to variations in the real components of the respective complex moduli of the different materials[20–22].

We imaged samples of Mylar D using FMM under a variety of imaging conditions, in order to evaluate the nature of the information which modulation techniques may provide concerning the local properties of the film around the silicate particles. *Figure 8* shows FMM images of a single particle (a) and a larger feature (b) thought from its topographical image (c) to be a cluster of smaller particles. In *Figure 8a*, the perimeter of the silicate particle is clearly delineated by a ring of high contrast. In *Figure 8b* the three particles of which the

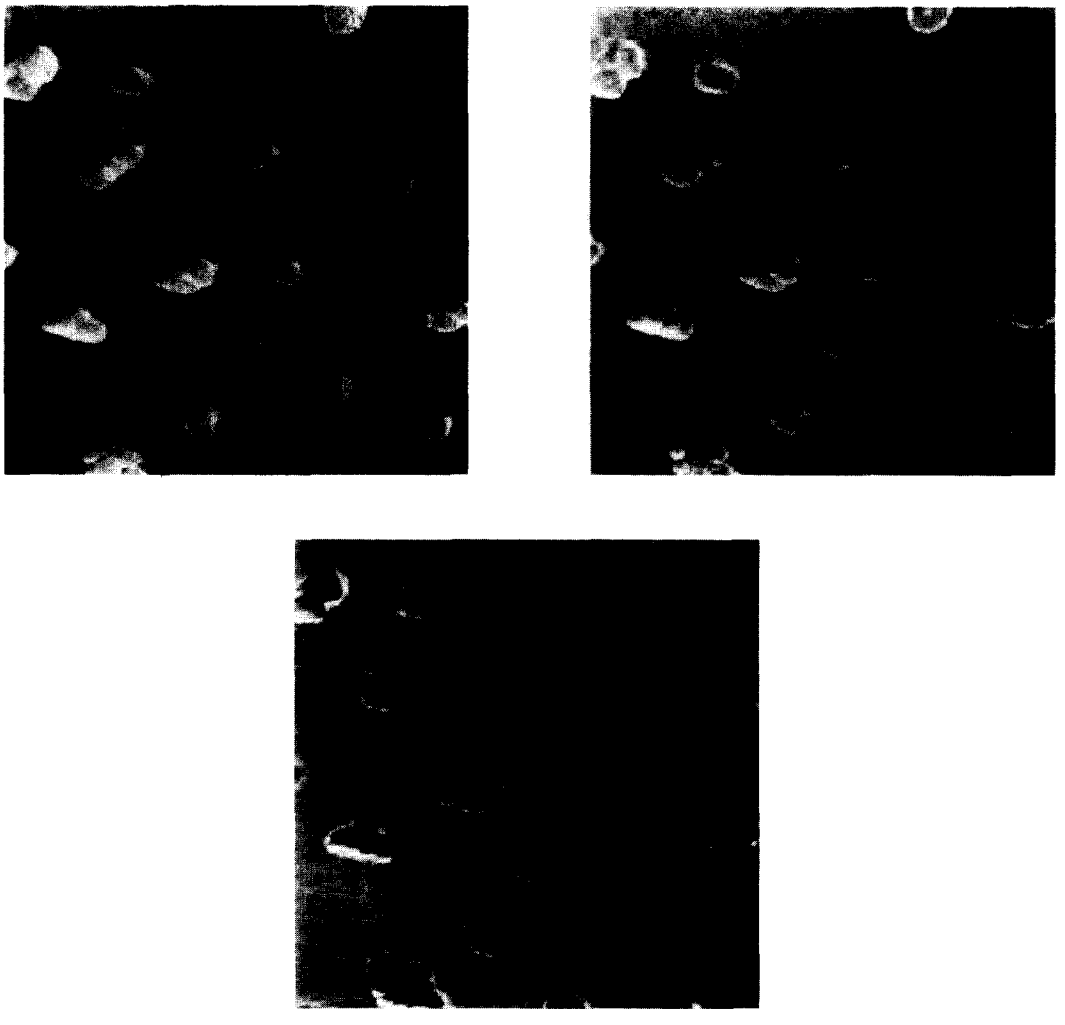

Figure 9 FMM images of Mylar D recorded at varying amplitudes of oscillation: 3 Å (a), 10 Å (b) and 40 Å (c). Image size: 3 μm × 3 μm. Scan speed 5 μm s^{-1}

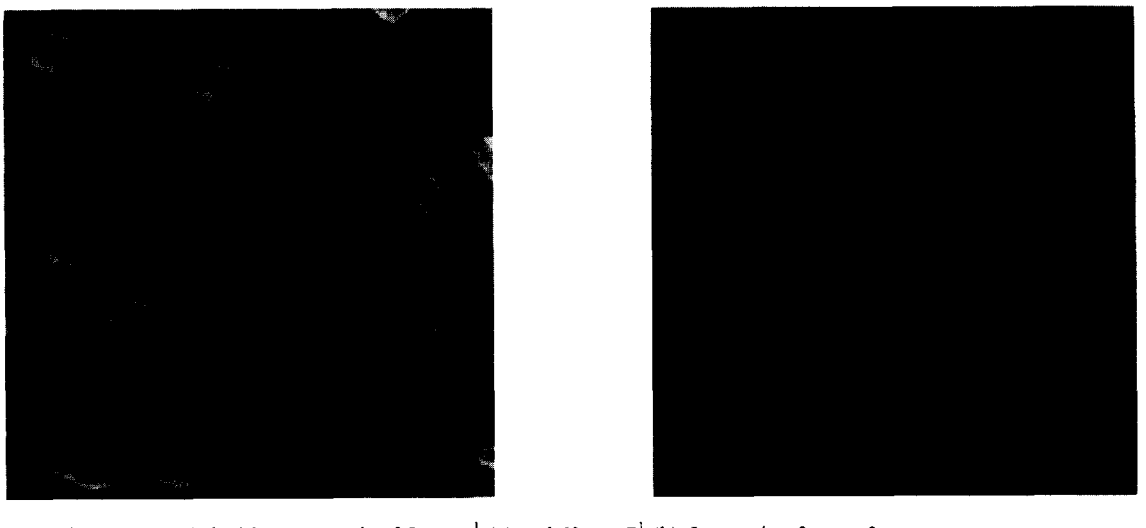

Figure 10 FMM images recorded with scan speeds of 5 μm s^{-1} (a) and 60 μm s^{-1} (b). Image size: 3 μm × 3 μm

cluster is composed are clearly identified. FMM has therefore assisted in confirming that some of the larger additive particles were indeed clusters of smaller ones. However, these data are in other respects difficult to interpret. According to the conventional interpretation of contrast in FMM, these data would imply increased stiffness around the perimeters of the additives. Furthermore, the slightly lower contrast observed over the majority of the exposed additive material in *Figure 8* would suggest a lower modulus for the silicates than for the polymeric matrix. Given our existing knowledge of the materials, this inference seems to be unsound: the modulus of the silicate would be *ca* 70 GPa while that of the polymer would be at least an order of magnitude lower. We must therefore seek an alternative explanation for the observed contrast in FMM mode.

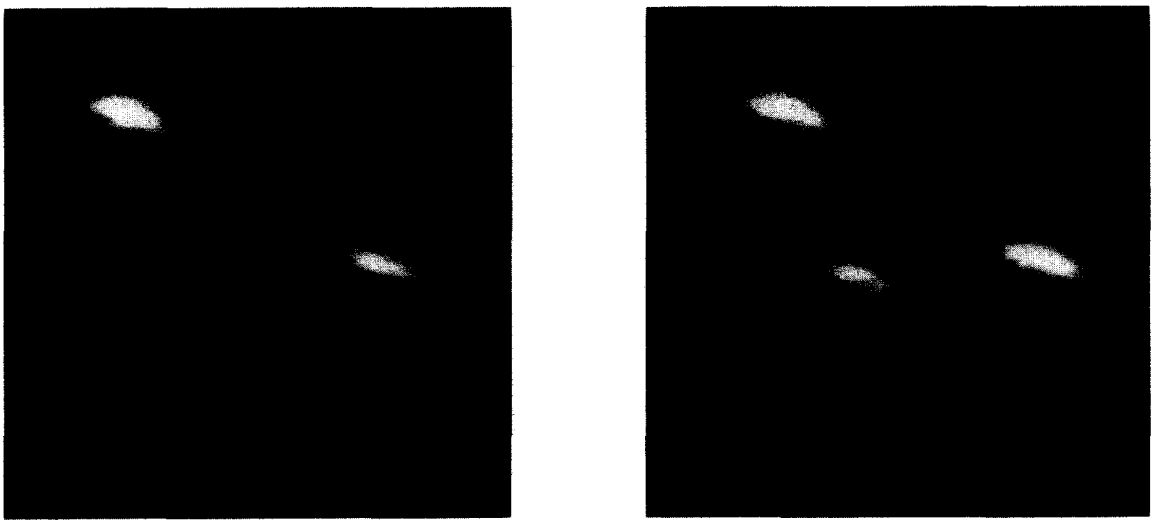

Figure 11 Forwards (a) and reverse (b) direction FMM images of colloidal gold particles deposited on mica. Image size: (a) 353 nm × 353 nm; (b) 376 nm × 376 nm

Significantly, samples of Mylar D were not flat in the regions occupied by the silicate additives—i.e. in the regions where variations in the local modulus might be expected. The data reported for polymeric materials by other workers[20–22] are for samples without pronounced protrusions, and it may be that sample curvature exerts a pronounced influence over FMM contrast. It is possible that the SFM tip interacts more forcefully at the bulk/particle interface because of the increased surface area in contact with the tip. However, this is a speculative explanation, and we have therefore performed a series of experiments designed to test the nature of the dependence of FMM contrast on sample topography and imaging conditions for Mylar D samples.

Contrast in FMM mode is influenced by both the amplitude of oscillation and the scan rate. *Figure 9* compares FMM images recorded with oscillation amplitudes of 3, 10 and 40 Å. At 40 Å, the silicates exhibit lower contrast than the surrounding polymer, but their perimeters are delineated clearly with high contrast. At 10 Å oscillation amplitude, the contrast difference between the silicates and the polymer has reduced, and the brightness of the particle perimeters has reduced. At 3 Å, the silicates now exhibit slightly higher contrast than the polyester, although increased contrast is still observed at particle boundaries. We are unsure of the explanation for this dependence of contrast on oscillation amplitude, and we are currently investigating the phenomenon further for other materials.

Figure 10 compares images recorded in FMM mode with a fixed amplitude of oscillation at 40 Å, and scan rates of 5 and 60 $\mu m\,s^{-1}$. Again, there is significant variation in contrast. At the lower scan speed, the silicates have higher contrast than the polymer, whereas at the higher scan speeds, the contrast is inverted (*Figure 10b*).

FMM images were recorded in the forward and reverse scan directions of colloidal gold particles deposited on mica (*Figure 11*). The gold particles exhibit relatively high contrast around their perimeters, reproducing the effect observed for the silicate particles (although in not quite such a pronounced fashion). Undoubtedly, the topography of the samples plays a role in causing these unexpected effects, and we intend to pursue further detailed investigations of the influence of sample topography on image contrast in FMM. No significant contrast differences were observed either for the gold particles or for the Mylar D specimens upon reversal of the scan direction in FMM.

CONCLUSIONS

Scanning force microscopy has proved to be a powerful tool for the characterization of polymer film topography. The resolution obtained in topographical mode SFM was superior to that observed in scanning electron micrographs of gold-coated specimens. The distribution and morphologies of silicate surface additives embedded in a polyester film material were characterized by both techniques. SFM revealed features which were absent from SEM images, including radiating structures which were observed around some of the larger silicate additives and which have been tentatively ascribed to strain-induced crystallization. SFM also provides the means by which local surface properties may be examined. LFM enabled imaging of local variations in the frictional characteristics of the sample material. Topographical contributions to the contrast in LFM were identified by comparing forward and reverse direction scanning. Gold colloids were observed to yield contrast which was purely topographical in origin, and which did not undergo an inversion on reversing the scan direction. However, silicate additives in Mylar D yielded high contrast in the forward direction LFM and were observed to undergo a contrast inversion in the reverse-direction image to appear as depressions. In FMM, the contrast was found to be complex in nature and influenced by a variety of experimental variables, including the scan rate and amplitude of oscillation. Furthermore, studies of colloidal gold particles confirmed that sample topography may also contribute to FMM image contrast. Further work is required in order to establish the dependence of FMM contrast on imaging conditions and sample topography before it may routinely be employed to probe the local properties of industrial film materials. However, SFM techniques more generally promise to make important contributions to our understanding of polymer film morphology and its dependence on processing variables.

ACKNOWLEDGEMENT

JSGL thanks the EPSRC for a research studentship. The authors are grateful to Nicola J. Bock for assistance with TEM characterization of the gold colloids.

REFERENCES

1. Bassett, D., *Developments in Crystalline Polymers*. Cambridge University Press, 1981, Ch 1.
2. Lin, F. and Meier, D. J., *Langmuir*, 1994, **10,** 1660.
3. Stocker, W., Schumacher, M., Graff, S., Lang, J., Wittman, J. C., Lovinger, A. J. and Lotz, B., *Macromolecules*, 1994, **27,** 6948.
4. Magnov, S. N. and Cantow, H.-J., *Journal of Polymer Science: Applied Polymer Symposium*, 1992, **51,** 3.
5. Miles, M. J., Jandt, K. D., McMaster, T. J. and Williamson, R. L., *Colloid Surfaces, A*, 1994, **87,** 235..
6. Hamers, R. J., Tromp, R. M. and Demuth, J. E., *Physics Reviews Letters*, 1986, **56,** 1972.
7. Ducker, W. A., Senden, T. J., Pashley, R. M., *Langmuir*, 1992, **8,** 1831.
8. Lee, G. U., Kidwell, D. A. and Colton, R. J., *Langmuir*, 1994, **10,** 354.
9. Lee, G. U., Chrisey, L. A. and Colton, R. J., *Science*, 1994, **266,** 771.
10. Wilbur, J. L., Biebuyck, H. A., MacDonald, J. C. and Whitesides, G. M., *Langmuir*, 1995, **11,** 825.
11. Overney, R. and Meyer, E., *MRS Bulletin*, 1993, May, 26.
12. Nisman, R., Smith, P. and Vancso, J. G., *Langmuir*, 1994, **10,** 1667.
13. Smith, P. F., Nisman, R., Ng, C. and Vancso, G. J., *Polymer Bulletin*, 1994, **33,** 459.
14. Maivald, P., Butt, H. J., Gould, S. A. C., Prater, C. B., Drake, B., Gurley, J. A., Elings, V. B. and Hansma, P. K., *Nanotechnology*, 1001, **2,** 103.
15. Burnham, N. A., Kulik, A. J., Gremaud, G., Gallow, P.-J. and Oulrbry, F., *Journal of Vacuum Science Technology*, 1996, **B14,** 794.
16. Ling, J. S. G., Murray, A. J. and Leggett, G. J., in preparation.
17. Grefstrom, S., Neitzert M., Hagen, T., Ackerman, J., Neumann, R., Probst, O. and Wortge, M., *Nanotechnology*, 1993, **4,** 143.
18. Haugstad, G., Gladfelter, W. L., Weberg, E. B., Weberg, R. T. and Jones, R. R., *Langmuir*, 1995, **11,** 3473.
19. Wiesendanger, R., *Scanning Probe Microscopy and Spectroscopy*. Cambridge University Press, Cambridge, 1994.
20. Kajiyama, T., Tanaka, K., Ohki, I., Ge, S.-R. Yoon, J.-S. and Takahara, A., *Macromolecules*, 1994, **27,** 7932.
21. Tanaka, K., Yoon, J.-S., Takahara, A. and Kajiyama, T., *Macromolecules*, 1995, **28,** 934.
22. Kajiyama, T., Ohki, I., Tanaka, K., Ge, S.-R. and Takahara, A., *Proceedings of the Japanese Academy*, 1995, **71B,** 75.